*Acta Cryst.* (1970). B26, 998

# Crystallographic Studies on Lactate Dehydrogenase at -75°C

BY DAVID J. HAAS* AND MICHAEL G. ROSSMANN

*Department of Biological Sciences, Purdue University, Lafayette, Indiana* 47907, *U.S.A.*

(*Received* 14 *July* 1969)

Crystals of lactate dehydrogenase (LDH) were frozen by equilibration in a sucrose–ammonium sulfate solution, and then dipping into liquid nitrogen. The rate of radiation damage for frozen crystals was tenfold less than for crystals at room temperature. The physical properties of frozen crystals are discussed. Analysis of 3·5 Å data collected at −75°C for native LDH and two heavy atom derivatives showed that these derivatives retained their isomorphism in the frozen state.

## Introduction

Radiation damage to protein crystals has been a problem in many protein structure determinations. Most protein crystals show a significant decrease in the average diffracted intensity after twenty-four hours of normal radiation exposure. Crystals are usually replaced when the intensity of suitably chosen reference reflections has declined by ten per cent or less, thus necessitating the use of many crystals for a complete high resolution data collection. Apart from the wasted time and material, caution has to be exercised in combining data from the various crystals owing to different absorption corrections and variations in heavy-atom substitution.

The most extensive crystallographic study of radiation damage was reported by Blake & Phillips (1962) in a study of myoglobin, but even here no direct information on the cause of the changes in the crystal was obtained. It is usually assumed that X-radiation produces sufficient free radicals in the liquid regions of the crystal to cause specific chemical changes on the surface of the protein molecules which then result in a general disordering of the crystal lattice (Strandberg, 1968). If this hypothesis is correct, the freezing of the mother liquor in the crystal's interstices would retard the transport of the free radicals throughout these regions. Unfortunately, freezing of protein crystals normally leads to crystal cracking owing to the differences in volume of the included water and ice (Low, Chen, Berger, Singman & Pletcher, 1966) and, thus, to a gross deterioration of the diffraction pattern. Recently Haas (1968) succeeded in freezing glutaraldehyde cross-linked lysozyme crystals soaked in 50% glycerol without apparent ill effects to the single crystals. This method was inapplicable to dogfish lactate dehydrogenase (LDH) crystals as they were destroyed by the cross-linking procedure. However, LDH crystals could be frozen after soaking them in a concentrated sucrose solution. We have demonstrated that such freezing does not seriously damage the crystal, and reduces the rate of radiation damage considerably.

Some of the properties of cold sucrose-filled LDH crystals are reported here. A complete low-temperature study was not feasible at this time owing to the demand on equipment for completing the room-temperature LDH study (Adams, Haas, Jeffery, McPherson, Mermall, Rossmann, Schevitz & Wonacott, 1969). Nevertheless, sufficient data were collected to show that reasonable isomorphism had been obtained for frozen crystals, and that a tenfold reduction in the rate of radiation damage had been achieved.

## Crystal preparation and physical properties

Selection of a solvent suitable for preparing crystals for rapid freezing was based on its glass-forming properties (Meryman, 1966) and its inability to denature proteins (Tanford, 1968). The latter requirement eliminated most normal anti-freeze compounds like glycol, glycerol and methanol. Ice-preventing compounds are particularly water soluble owing to their abundance of hydroxyl groups. Sucrose was selected as a compound which would be likely to prevent ice formation; it is also commonly used in high concentration in protein solutions without adverse effect.

Native dogfish LDH crystals can be grown from 2·0 *M* ammonium sulfate solution at *p*H 7·6 (Pesce, Fondy, Stolzenbach, Castillo & Kaplan, 1967). The crystals were prepared for freezing by dialysis against a solution containing 2·0 *M* ammonium sulfate and 3 *M* sucrose. They were placed in a cylindrical vessel covered on the bottom with a dialysis membrane and on the top by 'parafilm' (Lipscomb, Coppola, Hartsuck, Ludwig, Muirhead, Searl & Steitz, 1966). During the forty-eight hour equilibration period, the vessel was floated on the continuously stirred sucrose–ammonium sulfate solution.

It was found essential to freeze the protein crystals fast and isotropically. Anisotropic cooling resulted in mosaic qualities that varied with direction, or even complete disintegration of the crystal. Isotropic cooling was difficult to accomplish with the crystals mounted

* Present address: Philips Electronic Instruments, Mt. Vernon, N.Y. 10550, U.S.A.

in a capillary because of the flow of heat towards the crystal face in contact with the capillary surface. Cooling in a jet of cold gas was equally unsuitable because of more rapid cooling of the crystal faces near the gas jet. Thus, the usual mounting procedure consisted of placing a single LDH crystal (approximately 0·5 mm on each edge) on a strip of filter paper with a dropper, waiting until the liquid had been drawn off by the paper, scooping the crystal up on the end of a 0·25 mm glass fiber, and immediately plunging it into, and retaining it in, liquid nitrogen. The crystal was now frozen to the fiber and completely immobile. As the fiber had previously been mounted and aligned on the goniometer head, the crystal was also nearly centered for the diffractometer. Finally it was transferred quickly from the Dewar full of liquid nitrogen to the diffractometer where a jet of cold nitrogen gas prevented thaw. The cold jet of gas was always kept at a temperature lower than −60 °C in order to keep the sucrose solution in a solid glassy state. Ice formation was prevented both by use of a co-axial room-temperature nitrogen jet (Post, Schwartz & Fankuchen, 1951) and by surrounding the whole diffractometer with a dry-nitrogen filled polyethylene bag.* This cover was supported by a circular wooden frame above the instrument, equal in diameter to the diffractometer table. It was gathered below the table, and also firmly pressed to its edges, by stretched rubber tubing to prevent excessive loss of gas. The high tension and other cables entered through a hole which was plugged with glass wool. The supply of dry nitrogen maintained a slightly higher pressure within the enclosure and hence helped prevent back diffusion of moist air. Liquid nitrogen consumption was 1·5 liters per hour. A thermocouple placed near the end of the cold jet provided a continuous record of the crystal temperature.

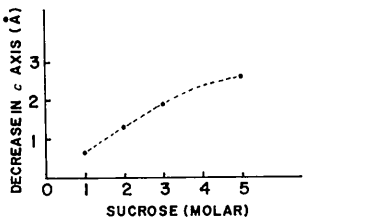


Fig. 2. Change in length of *c* axis of frozen crystals with sucrose concentration.

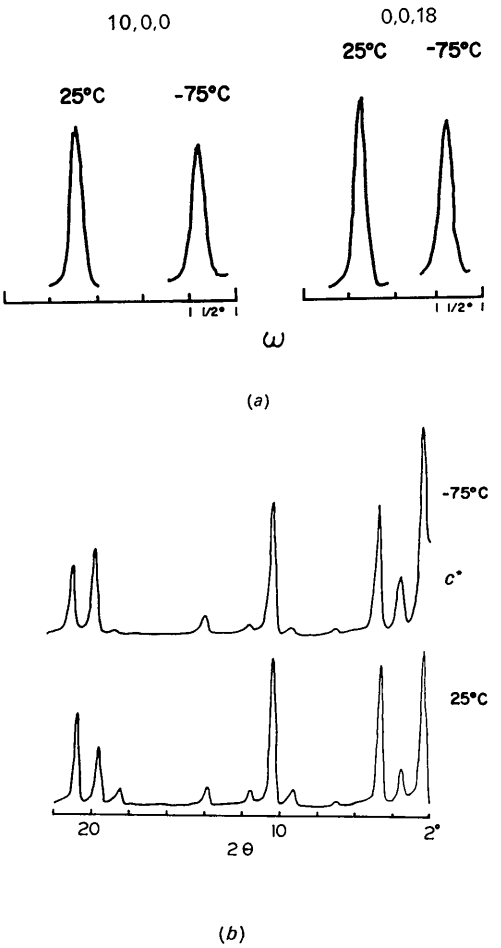


Fig. 3. Comparison of traces to show quality of crystals in 3*M* sucrose before and after freezing: (*a*) $\omega$-scans of the 10,0,0 an 0,0,18 reflections (*b*) $2\theta$-scans of the 00*l* reflections.

The presence of 3*M* sucrose in the crystal at room-temperature causes some intensity changes, particularly to the low order reflections [Fig. 1(*a*) and (*b*)], which presumably is due to the change in electron density between the protein molecules. No change in lattice constants could be observed with the addition of sucrose prior to freezing. However, on freezing the crystals, the cell dimensions decrease by an amount roughly proportional to the sucrose concentration (Fig. 2 and Table 1). The consequent alteration in the sampling position of the molecular transform causes further high-order intensity changes [Fig. 1(*b*) and (*c*), and also Fig. 3(*b*)]. No appreciable intensity changes were observed with variation in temperature between −75 and −125 °C.

Table 1. *Lattice constants of room temperature and cold* LDH *crystals* (3*M sucrose*)

| | 25 °C | −75 °C |
|---|---|---|
| Space group | *F*422 | *F*422 |
| *a* | 146·5 Å | 145·0 Å |
| *c* | 155·1 | 153·1 |
| *Z* | 8 | 8 |

The diffraction quality of the frozen crystals improved as the sucrose concentration increased. When a concentration of 3*M* sucrose had been attained there was little difference between the quality of the crystals

* We thank W. N. Lipscomb who suggested such an enclosure.

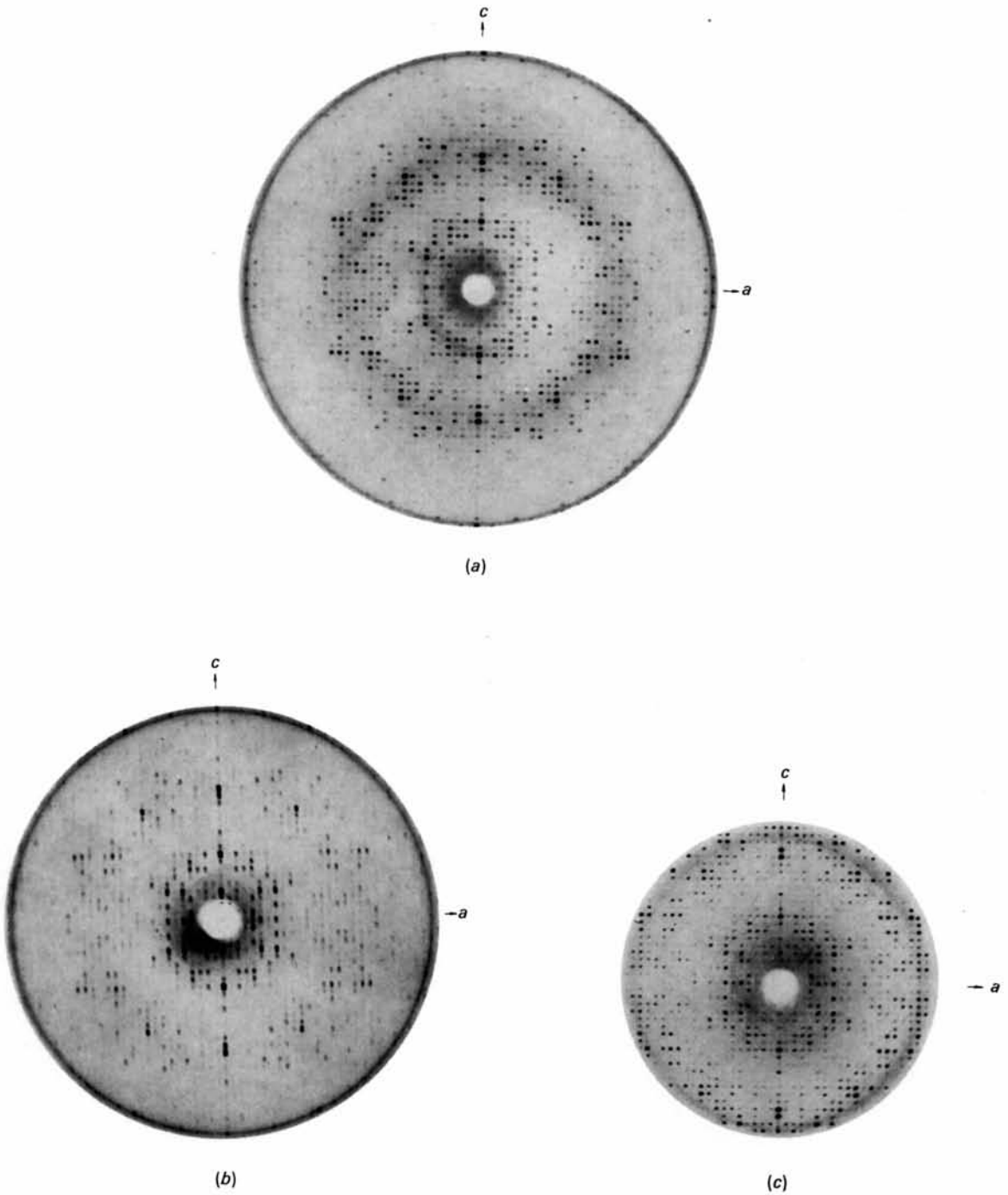


Fig. 1. Precession photographs of the *h*0*l* zone of (*a*) native LDH crystals at room-temperature ($\mu = 18°45'$); (*b*) sucrose-soaked LDH crystals also at room-temperature ($\mu = 17°0'$); and (*c*) frozen sucrose-soaked LDH crystals at $-75°C(\mu = 12°0')$. Intensity differences between (*a*) and (*b*) are principally in the low order reflections. The intensity distribution of (*c*) differs from that of (*a*) in the higher order reflections.

[*To face p.* 999

at room temperature and in the frozen state [Fig. 3(*a*)]. Bragg reflections of crystals soaked in less than 2*M* sucrose were so broad and irregular that accurate lattice constants were difficult to measure. The 0,0,36 reflection (Fig. 4) is particularly sensitive to increasing sucrose concentration: it also shows intensity changes caused by the presence of sucrose and the decrease in the length of the *c* axis. A 3·0 *M* concentration of sucrose was therefore found to be a reasonable compromise between adequate crystal perfection and limited changes in lattice constants.

A comparison of the effect of radiation damage on the cold and room-temperature crystals is shown by a plot of the reference reflections 10,0,0 and 0,0,18 at regular intervals of exposure time (Fig. 5). Whereas the intensities from room-temperature crystals had usually decayed by 10% of their original value within 30 hours, cold crystals took more than 300 hours to reach the same point. Irregularities in the decay curve of the cold crystal are primarily due to extra absorption of ice which formed occasionally. The presence of some residual decay in the cold crystals could be attributed to disordering caused by a reduced amount of free radical activity or to disordering of the crystal lattice caused by sublimation of ice from the crystal interior. As the relative rate of decrease of the two reference reflections remained the same, although the absolute rate had been decreased, a similar cause for decay should probably be attributed at both temperatures.

The 1·5% changes in lattice constants in 3*M* sucrose made it necessary to consider the cold, sucrose-filled, crystals as a different system from that of the room-temperature crystals. Hence, any investigation of heavy-atom derivatives had to be carried out relative to 'cold native' data.

### Data collection and phase refinement

Three dimensional 3·5 Å resolution X-ray intensities were collected for cold native LDH and for two heavy-atom LDH derivatives: dimercury acetate (DMA) and Baker dimercurial (BDM). Both of these derivatives had also been used in the room temperature study (Adams *et al.*, 1969). These two compounds substitute principally the most reactive sulfhydryl 'A' site on each polypeptide chain.

A card-controlled Picker four-circle diffractometer was used according to the system described by Adams *et al.* (1969). However, cylindrical rather than ellipsoidal absorption corrections were applied, and crystals with their *a* or *c* axes parallel to the diffractometer $\varphi$ axis, rather than only the latter, were utilized in this work. Intensities were measured through an $\omega$-scan (moving crystal–stationary counter) of 0·7°, in preference to a $2\theta$ scan (moving crystal–moving counter) which would not have given sufficient resolution of Bragg maxima. Background was measured for twenty seconds on either side of the scan to give roughly equal time for peak and total background measurements. Two Friedel-related observations were made of each independent reflection. Although only one crystal would have been necessary in collecting the data on each compound, accidents required the use of five

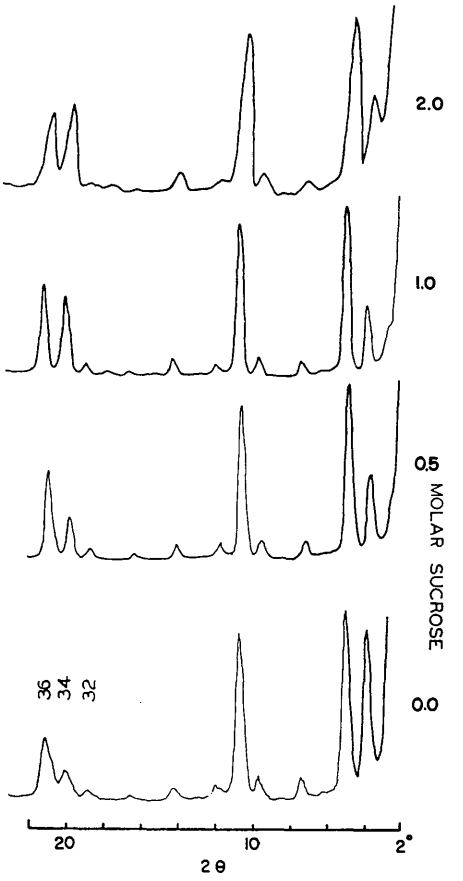


Fig. 4. Traces given by $2\theta$-scans of frozen crystals with different sucrose concentrations. The quality of the crystals improves as the concentration increases. Note the progressive changes of intensity and width of the 0,0,32, 0,0,34, and 0,0,36 reflections. The criterion for crystal perfection was, however, judged principally on the basis of $\omega$-scans.

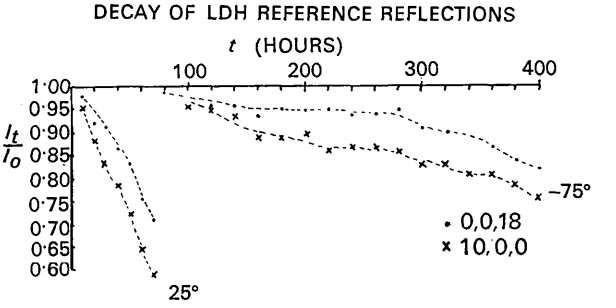


Fig. 5. The ratio $I_t/I_0$ for two reference reflections plotted as a function of exposure time for a typical native and frozen crystal. $I_t$ represents the intensity at time $t$. Results for 0,0,18 and 10,0,0 are shown with dots and crosses respectively.

crystals for both the native and dimercury acetate data collection. The polyethylene bag covering the whole diffractometer was not introduced until the Baker dimercurial data collection. Hence some inaccuracies were encountered owing to ice formation for the native LDH and DMA but not for the BDM measurements. Consequently, all reflections for which the Friedel-related measurements differed by more than 300 electrons were omitted. The mean $F$ was 1600 electrons on the same approximate absolute scale. The final number of acceptable native intensities was 3957 out of a possible 5100 independent reflections with spacing greater than 3·5 Å. Almost 3000 of these measurements were matched with measurements of structure amplitudes from both DMA and BDM, while the remainder had only one matching heavy atom derivative intensity.

The $R$ value,

$$= \sum_{\text{reflect.}} \sum_{\text{crystals}} |(F_{\text{mean}} - F_{\text{obs}})| / \sum \sum F_{\text{mean}} ,$$

of fifteen scaling reflections between five different native crystals was 1·8% compared with an $R$ value of 0·84% obtained from the same reflections between five different room-temperature native crystals. The scaling and fitting of the heavy atom data sets to the cold native data, the computation of difference Patterson and electron density maps, and the least-squares refinement were executed with the same computer programs as those used in the room-temperature work (Adams *et al.*, 1969). The low-temperature data were put on a scale corresponding to that of the room-temperature data by equating the average value of the two data sets. The constant term in the quadratic scaling expression $F' = (a + bF + cF^2) \exp\left(-B \frac{\sin\theta^2}{\lambda^2}\right)$ was assumed zero and the values of $c$ were found to be negligibly small. Table 2 compares the temperature factors and root-mean-square differences between the native LDH and each of the two heavy-atom derivatives for the room-temperature and frozen crystals. The quadratic constants and temperature factor $B$, as quoted in Table 2, were applied to the derivative data to make them correspond to the native data.

Fig. 6 shows the 4 Å resolution Harker section $z = 0$ through the $(|F_{PH}| - |F_P|)^2$ difference Patterson (Rossmann, 1960) for both heavy-atom compounds using the low-temperature data and, for comparison, the corresponding room-temperature map at roughly 4·0Å (DMA) and 5·0 Å (BDM). The cold temperature BDM peak is rather small owing to the low occupancy of the heavy atom in the crystal used for the data collection. Fig. 7 shows the anomalous dispersion DMA Patterson with $(F_h - F_{\bar{h}})^2$ coefficients (Rossmann, 1961). For comparison, the corresponding room-temperature 4·0 Å anomalous dispersion Patterson is also shown. The significant features along the axes and diagonal are easily recognizable for the room temperature results. The cold temperature results show the same features but less significantly due to larger experimental error in the intensity measurements.

Initially the refinement was restricted to 5 Å resolution data, (Dickerson, Kopka, Varnum & Weinzierl, 1967) without anomalous dispersion, to establish values for the occupancies and temperature factors. Subsequently all 3·5 Å data were included in the refinement. Unfortunately both heavy-atom derivatives were rather similar in that they both substituted at site '*A*'. Furthermore the position of this site is somewhat special ($x \simeq y$). Thus the phases clustered around 0 and $\pi$ before the introduction of anomalous dispersion into the refinement. No independent decision on the enantiomorph could be taken on the basis of the DMA and BDM data alone. Indications of the correct enantiomorph could therefore be obtained either by matching each of the two possible electron density maps with the room-temperature work, or by accepting the previously determined hand for the room-temperature crystals.

The least-squares refinement performed with the anomalous dispersion applied with either sign gave essentially identical $R$ values and distributions of the figures of merit. Because of the bimodal character of the phase diagrams before the anomalous dispersion was added, the mean figure of merit was 0·49, but rose to 0·64 as a consequence of the selection of one of the two modes on each set of phase circles. Comparison of the occupancy and shape parameters at the two temperatures shows that the DMA behaves similarily in both cases, although its apparent occupancy at the lower temperature is somewhat greater. The BDM derivative parameters further confirm its only partial substitution (Table 3). Lack of good resolution of the latter's subsidiary *A*-site gave rise to some problems in refinement as is apparent by the large temperature fac-

Table 2. *Results of the least-squares fit to remove systematic errors and to place the data from all derivatives on a similar, approximately absolute scale*

| Compound | $n$ (number of reflections) | r.m.s. difference from native LDH $\sqrt{[\Sigma(F_{PH} - F_H)^2/n]}$ (electrons) | Temperature factor $B$ (Å²) |
|---|---|---|---|
| DMA | | | |
| 25°C | 3985 | 137 | −5·9 |
| −75°C | 3422 | 337 | −12·2 |
| BDM | | | |
| 25°C | 2038 | 151 | −13·3 |
| −75°C | 3440 | 179 | −6·6 |

Table 3. *Final heavy atom parameters from least-squares phase refinement*

3·5 Å resolution for cold crystal data; 4 Å resolution for room-temperature DMA; 5 Å resolution for room-temperature BDM.

$Z$ is the occupancy of each atom in electrons on the roughly absolute scale. $x,y,z$ are the positional parameters of the atoms. $B$ is the isotropic shape parameter of an atom in Å$^2$. Figures in parentheses show mean isotropic equivalent in case of anisotropic refined values. $\beta_{hh}\ldots\beta_{ll}$ are the six dimensionless anisotropic shape parameters. $\Delta f''/(f+\Delta f')$ is the ratio of the imaginary to real anomalous scattering component as determined by the least-squares procedure.

| Compound | Site | $Z$ | $x$ | $y$ | $z$ | $B$ | $\beta_{hh}$ | $\beta_{kk}$ | $\beta_{ll}$ | $\beta_{hk}$ | $\beta_{kl}$ | $\beta_{lh}$ | $\Delta f''/(f+\Delta f')$ |
|---|---|---|---|---|---|---|---|---|---|---|---|---|---|
| DMA | | | | | | | | | | | | | |
| 25°C | *A* | 87·0 | 0·134 | 0·138 | 0·229 | (180) | 0·0011 | 0·0042 | 0·0006 | 0·0053 | −0·0010 | 0·0021 | +0·09 |
| | *A'* | 13·5 | 0·150 | 0·148 | 0·197 | 113 | | | | | | | |
| −75°C | *A* | 156·5 | 0·132 | 0·140 | 0·229 | (90) | 0·0010 | 0·0018 | 0·0003 | 0·0042 | −0·0013 | −0·0018 | +0·11 |
| BDM | | | | | | | | | | | | | |
| 25°C | *A* | 81·6 | 0·140 | 0·147 | 0·224 | 64 | | | | | | | +0·09 |
| | *A'* | 36·8 | 0·148 | 0·148 | 0·189 | 261 | | | | | | | |
| −75°C | *A* | 58·8 | 0·133 | 0·143 | 0·227 | (18) | −0·0002 | 0·0006 | 0·0002 | 0·0030 | −00·012 | −0·0012 | +0·18 |

tors. Table 4 defines and lists various residuals for each of the two compounds at the end of refinement. The generally significantly larger size of $\langle f \rangle$ in comparison with the lack of closure error $E_\theta$ can be taken as a sign

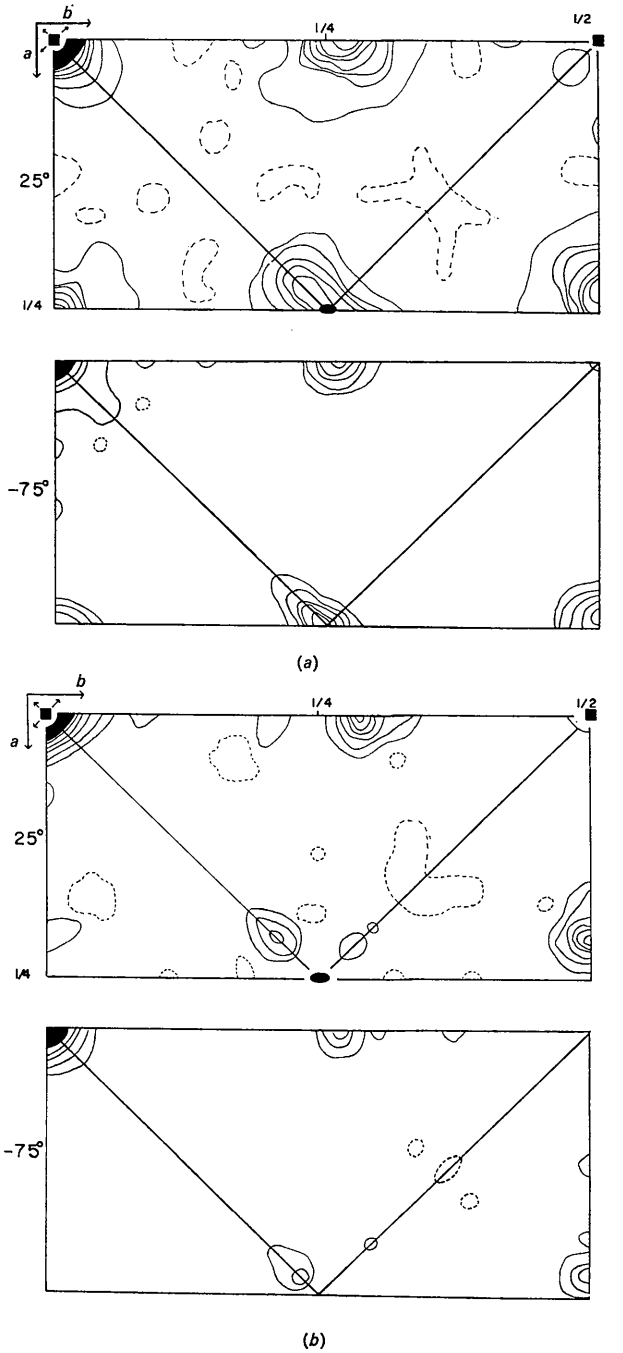


Fig. 6. Harker sections for (*a*) DMA and (*b*) BDM at $z=0$ of the difference Patterson maps, with $(|F_{PH}|-|F_P|)^2$ as coefficients, for room-temperature data (above) and −75°C data (below). Origin heights on corresponding room-temperature and −75°C maps were scaled to the same contour level.

of reasonably good isomorphism. The improved residuals with increased resolution is most probably an artifact caused by the presence of only two rather similar heavy-atom derivatives in the refinement.

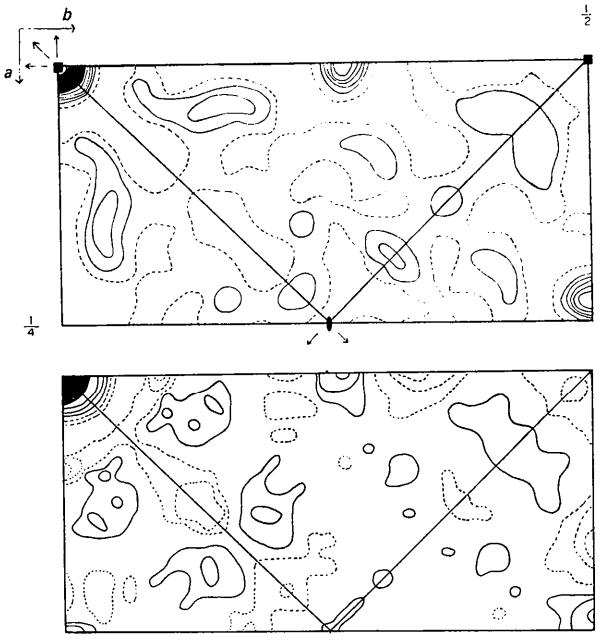


Fig. 7. Sections $z=0$ for the DMA anomalous dispersion Patterson syntheses with $(F_h-F_{\bar{h}})^2$ coefficients. The room-temperature map is above while the results from data collected at $-75$ °C are shown below. The significant features along the axes (double weight peak) and on the diagonal (single weight peak) are easily recognizable at room temperature. These features are still recognizable for the cold temperature work although they are much closer to background noise.

Two 5 Å electron-density maps were computed from the cold-crystal data, each representing one of the two ways the anomalous dispersion could be introduced. A comparison of these maps with the 5 Å room-temperature LDH map showed that one had more features in common with the room-temperature results. This map, while still showing considerable discrepancies, corresponded to the same enantiomorph selected for the room-temperature study. Fig. 8 (section $z=\frac{12}{80}$) shows one of the better-matched sections. A 3.5 Å electron-density map was computed with the now correctly established sign of the anomalous dispersion. This map showed numerous discontinuous regions of positive density and compared more poorly with the corresponding, tentative, room-temperature 4 Å electron-density map. As the cold temperature work is based only on a virtually single isomorphous replacement set, the comparison of the room and low-temperature results is similar to that made between maps based on a single isomorphous and multiple isomorphous phase determination for hemoglobin (Blow & Rossmann, 1961). The refinement of the mean lack of closure given in Table 4 suffers from the same basic problem, although the results, particularly for BDM, are not dissimilar to those of Adams *et al.* (1969).

It would seem reasonable to expect, on the basis of the preliminary investigation reported here, that, with the inclusion of further heavy-atom compounds, frozen LDH crystals are likely to yield a satisfactory electron density distribution. These crystals have the advantage of a tenfold reduction in the rate of radiation damage as well as the elimination of background scattering due to the glass capillary and liquid surrounding the crystal. However, the overall 'temperature' factor remains substantially unaltered. The inconvenience and ex-

Table 4. *Final errors in refinement procedure*

(See Adams *et al.*, 1969)

| Compound | Criterion | 15·4 | 7·7 | 5·1 | 3·9 | 3·1 |
|---|---|---|---|---|---|---|
| | | | | Resolution in Å | | |
| DMA | $E_\theta$ | 570 | 302 | 154 | 206 | 207 |
| | $\langle f \rangle$ | 525 | 401 | 375 | 413 | 521 |
| | $\langle (F_{PH}-F_P) \rangle$ | 770 | 472 | 286 | 298 | 367 |
| | $k$ | +0·206 | +0·132 | +0·101 | +0·101 | +0·124 |
| | $n$ | 73 | 460 | 833 | 1322 | 462 |
| BDM | $E_\theta$ | 171 | 138 | 108 | 94 | 279 |
| | $\langle f \rangle$ | 203 | 179 | 196 | 263 | 513 |
| | $\langle (F_{PH}-F_P) \rangle$ | 257 | 198 | 160 | 163 | 328 |
| | $k$ | +0·325 | +0·224 | +0·210 | +0·168 | +0·094 |
| | $n$ | 74 | 468 | 1085 | 1578 | 88 |
| All compounds together: | | | | | | |
| $R_1$ (modulus residual) | | 0·80 | 0·60 | 0·38 | 0·32 | 0·27 |
| $R_2$ (weighted residual) | | 0·73 | 0·44 | 0·19 | 0·16 | 0·15 |
| $m$ (figures of merit) | | 0·57 | 0·66 | 0·66 | 0·64 | 0·54 |
| $n$ (number of reflections) | | 74 | 473 | 1118 | 1811 | 481 |

$E_\theta$ represents r.m.s. lack of closure for given compound in phase diagram.
$\langle f \rangle$ is the mean structure amplitude of the heavy atom contribution.
$\langle F_{PH}-F_P \rangle$ is the mean difference between the heavy atom derivative and native structure amplitude.
$k=\Delta f''/(f+\Delta f')$ and represents the apparent size of the anomalous dispersion effect. For a mercury atom $k$ should be 0·10.
The $R$ values were normalized with sums over the heavy atom scattering amplitudes or their squares.
$R_1$ represents a modulus addition of the lack of closure error of the phase diagrams.
$R_2$ represents a sum of weighted squares over the same terms as $R_1$.

pense of liquid nitrogen cooling apparatus can probably be overcome by perfecting thermoelectric coolers which are presently available for temperatures down to −100°C. We are testing one of these in our laboratory.

We wish to express out thank to Drs M. J. Adams, H. Mermall, and A. Wonacott and Mr P. Lentz for their assistance and for making available their data processing programs. Thanks are also due to Mrs J. Jacobson for her able technical assistance. We are grateful to the Cancer Chemotherapy National Service Center for supplying the sample of Baker dimercural. This work was supported by NIH Grant GM-10704 and NSF Grant No. GB5477.

## References

ADAMS, M. J., HAAS, D. J., JEFFERY, B. A., MCPHERSON, A. JR, MERMALL, H. L., ROSSMANN, M. G., SCHEVITZ, R. W. & WONACOTT, A. J. (1969). *J. Mol. Biol.* **41**, 159.

BLAKE, C. C. F. & PHILLIPS, D. C. (1962). *Biological Effects of Ionizing Radiation at the Molecular Level.* Symposium, International Atomic Energy Agency, Vienna.

BLOW, D. M. & ROSSMANN, M. G. (1961). *Acta Cryst.* **14**, 1195.

DICKERSON, R. E., KOPKA, M. L., VARNUM, J. C. & WEINZIERL, J. E. (1967). *Acta Cryst.* **23**, 511.

HAAS, D. J. (1968). *Acta Cryst.* B**24**, 604.

LIPSCOMB, W. N., COPPOLA, J. C., HARTSUCK, J. A., LUDWIG, M. L., MUIRHEAD, H., SEARL, J. & STEITZ, T. A. (1966). *J. Mol. Biol.* **19**, 423.

LOW, B. W., CHEN, C. C. H., BERGER, J. E., SINGMAN, L. & PLETCHER, J. F. (1966). *Proc. Nat. Acad. Sci. Wash.* **56**, 1746.

MERYMAN, H. T., Ed. (1966). *Cryobiology*, pp. 16–21, 239–242. New York: Academic Press.

PESCE, A., FONDY, T. P., STOLZENBACH, G., CASTILLO, F. & KAPLAN, N. O. (1967). *J. Biol. Chem.* **242**, 2151.

POST, B., SCHWARTZ, R. S. & FANKUCHEN, I. (1951). *Rev. Sci. Instrum.* **22**, 218.

ROSSMANN, M. G. (1960). *Acta Cryst.* **13**, 221.

ROSSMANN, M. G. (1961). *Acta Cryst.* **14**, 383.

STRANDBERG, B. (1968). *Ark. Kemi*, **28**, 1.

TANFORD, C. (1968). *Advanc. Protein Chem.* **23**, 122.

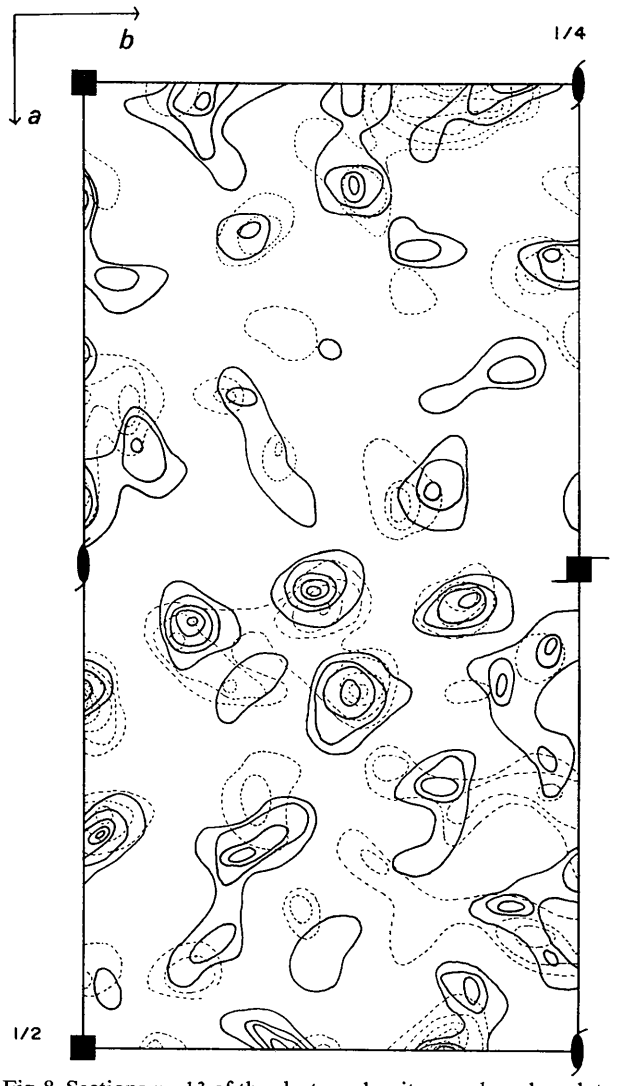


Fig. 8. Sections $z = \frac{1}{8}\frac{2}{0}$ of the electron density map based on data from two compounds collected at low-temperature superimposed on the five-compound room-temperature results (dashed). Only positive contours are shown. Changes in cell dimensions between the two temperatures have been neglected in the presentation of these results.